

Modeling a mixed SEP event with the PATH model: December 13, 2006

Olga P. Verkhoglyadova*, Gang Li^{*,†}, Gary P. Zank* and Qiang Hu*

**Institute of Geophysics and Planetary Physics, University of California, Riverside, Riverside, USA*

†*SSL, University of California, Berkeley, USA*

Abstract. There are often two particle components which form a major SEP event, one originating from a solar flare and the other from solar wind particles accelerated at a traveling CME-driven shock [1]. If a CME and a flare are part of the same process, then the interplay between corresponding energetic particle components may yield temporal, spectral, and compositional differences in observations. Depending on spacecraft location and magnetic connection to either a flare site or a CME-driven shock (or both), we expect to observe distinct signatures in the time intensity profiles. Following an approach by Li and Zank [2], we apply the Particle Acceleration and Transport in the Heliosphere (PATH) one-dimensional numerical code developed at University of California in Riverside to model the mixed SEP event of December 13, 2006. We initiate the code by modeling a quiet-time solar wind. Observed shock parameters at 1 AU and flare characteristics then are used as input into the code. We model energetic particle acceleration at a traveling quasi-parallel CME-driven shock and subsequent transport throughout the interplanetary medium to 1 AU. Time-intensity profiles and spectra of proton and heavy ions are presented and compared with in situ measurements by ACE. Contributions from the solar wind suprathermal and flare particles to the resultant SEP event are discussed.

Keywords: MHD, shock, particle acceleration, energetic particles

PACS: 52.30.Cv, 52.35.Tc, 52.65.Pp, 96.50.Pw, 96.50.Vg, 96.60.qd

OBSERVATIONS

The SEP event of December 13, 2006 has started with an X3.4 class flare with the maximum intensity registered by the X-ray detector onboard GOES-10 and GOES-12 satellites at 02:54UT. Duration of the flare was 43 minutes. A ground level event (GLE) was detected by neutron monitors on the ground. There was a halo CME event observed by SOHO. The SOHO LASCO CME Catalog provides an estimate for the CME linear speed as 1774 km/sec. The CME-driven shock reached 1 AU at about 14:00UT the next day and the corresponding ESP signatures were observed by the ACE satellite around that time. A summary of X-ray fluxes, energetic particle fluxes and magnetic field measurements by GOES, and neutron monitor measurements are presented in Figure 1 (courtesy of the National Geophysical Data Center, NOAA).

MODELING RESULTS

We apply the Particle Acceleration and Transport in the Heliosphere (PATH) code developed at IGPP at UCR to model the December 13, 2006 SEP event. First, we model the background solar wind plasma flow and then the evolving CME-driven shock

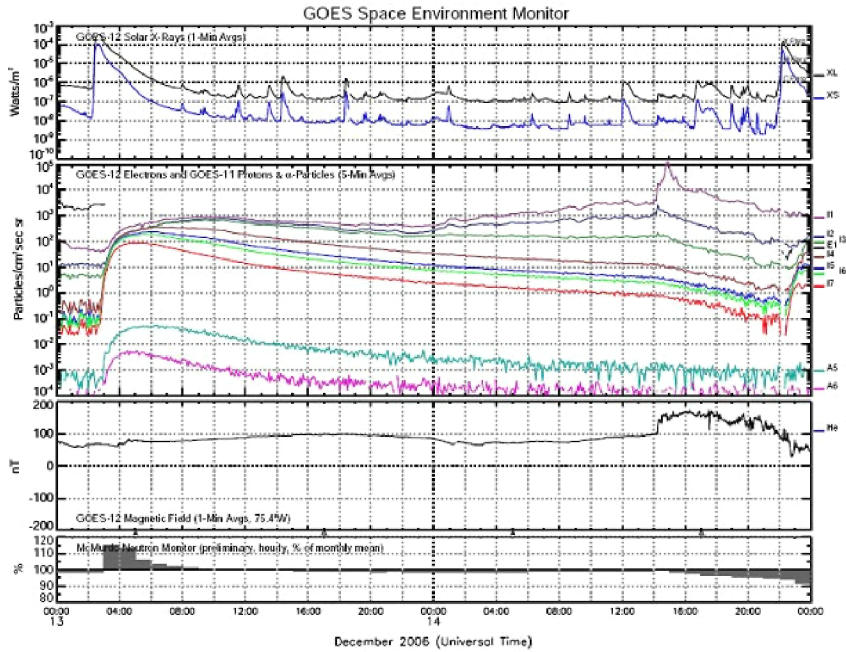


FIGURE 1. Data from the GOES Space Environment Monitor (SEM) for December 13 and 14, 2006. The data is provided by the NGDC, NOAA (<http://www.ngdc.noaa.gov/stp/GOES/goes.html>). Flare signatures on Dec. 13 at 04:00UT are seen in X-rays (top panel), particle fluxes (second panel from the top) and cosmic ray background increases in the neutron monitor measurements (bottom panel). The shock arrival on the next day at 14:00 UT are noted in both the particle fluxes and magnetic field measurements at the Earth’s orbit (second panel from the bottom).

propagating onto this background. We use the ACE measurements of magnetic field and plasma at 1 AU at the shock arrival time to extrapolate boundary conditions for the model. A parallel shock is launched at about 0.1 AU from the Sun. In the model, it is assumed that the shock remains in this quasi-parallel configuration throughout its propagation from the Sun to the Earth’s orbit. Estimates of the angle between the shock normal and interplanetary magnetic field show 30 degrees at 1 AU. The estimated parameters at 1 AU and modeling results are summarized in the Table 1.

In the next “particle block” of the PATH code particles from the solar wind suprathermal population (> 10 keV/nuc) are injected into the shock (the so-called “seed” particles), where they experience diffusive shock acceleration (DSA also known as first-order Fermi acceleration). The particles leave the shock, but get scattered by MHD turbulence in its vicinity, bounce back and cross the shock repeatedly. We assume a steady state

TABLE 1. Summary of MHD parameters estimated from the ACE measurements at 1 AU and obtained from modeling results.

	Compressional ratio	Upstream speed, km/sec	Shock speed, km/sec	Arrival time, hrs
Observations	3.0±0.3	650±30	800±50	35
Model	2.8	650	730	49

distribution function solution in the shock vicinity:

$$f \sim p^{-s(t_k)} (H(p - p_{inj}(t_k)) - H(p_{max}(t_k) - p)),$$

where the distribution function (f) is defined by particle momentum (p), injection momentum (p_{inj}), maximum local momentum cut-off (p_{max}) and the shock spectral index (s) at any given time step (t_k). We assume that the shock has enough time to accelerate all the particles involved in the simulation at each time step. The SEPs can be accelerated up to a 100 MeV/nuc at the shock before they escape. As the shock evolves and decelerates in the interplanetary medium, particle acceleration becomes less effective. Escaping particles scatter in pitch-angle along the interplanetary magnetic field lines. A Monte-Carlo approach is used to model particle transport between the shock and 1 AU and beyond. Output of the code are particle dynamical spectra, time-intensity profiles (fluxes) for protons and heavy ions and composition ratios. Details of the model are described in the papers [4, 5, 6, 3].

To model the mixed December 13, 2006 SEP event we need to include both solar wind suprathermals and flare particles into the seed population (see [1, 2]). We assume that the flare particles are injected into the shock in the energy range up to 1 GeV during the whole duration of the flare (~ 43 minutes). The flare particle momentum distribution is assumed to be $\sim p^{-4.5}$. We assume that the flare particles constitute 45% of the seed population. We assign an injection energy of 10 keV to the solar wind suprathermals with an ejection efficiency of 1% flux density.

Figure 2a and b present event-integrated spectra for iron and oxygen ions (from the beginning of the flare and launch of the CME-driven shock to the moment when the shock arrives at 1 AU). We assume that charge states for iron and oxygen were 16 and 6, correspondingly. The plots show the standard DSA power-law [7] and spectral breaks at high energies. We use ULEIS [8] and SIS [9] particle detectors to estimate integrated fluxes and spectra at 1 AU and compare with our results. The low-energy parts of the spectra are fitted to ULEIS measurements (shown by diamonds) and the high-energy part of the heavy ion spectra are fitted to the SIS measurements (shown by triangles). The modeled spectra are plotted in arbitrary units and are scaled to the observed flux magnitudes in the Figure. We use the same scaling factor for all energy channels. Since the integrated spectra result from overlaying a series of instantaneous spectra at different times, the cumulative spectrum reflects the weakening of the shock with time. The maximum energy to which a particle can be accelerated decreases as the shock propagates and only those high energy particles, that were trapped at an earlier

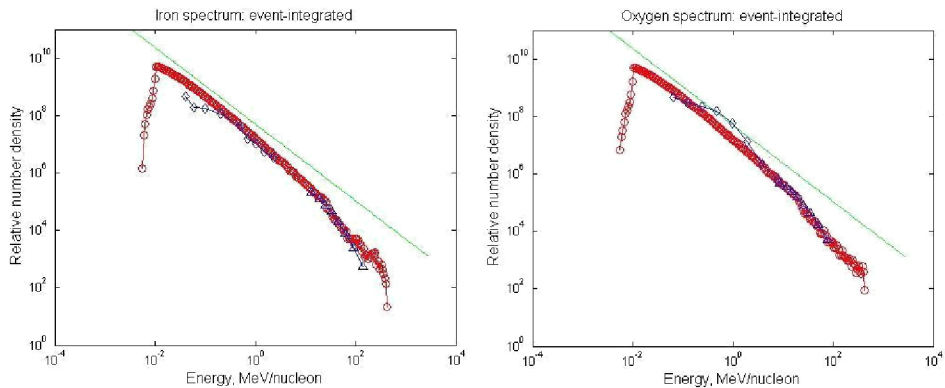


FIGURE 2. Event-integrated spectra for iron (left panel) and oxygen (right panel) ions are shown by the red circles. Theoretical power-law spectra at 1 AU are shown by solid lines. Diamonds and triangles (in blue) represent event-integrated measurements by ULEIS and SIS onboard ACE, correspondingly. Event duration is about 49 hrs.

time and then subsequently leaked out, contribute to the spectrum, resulting in a broken power-law feature. This trend is reflected in observations by SIS of iron and oxygen ions in the high-energy range up to 100 MeV/nucleon.

Figures 3 and 4 present modeled fluxes of iron and oxygen ions, correspondingly, at 1 AU. Left panels show fluxes for six representative energies in the high-energy range (from 13 to 140 MeV/nuc) and right panels show fluxes in the low-energy range (from 44 keV/nuc to 2 MeV/nuc) which approximately correspond to the ranges of SIS and ULEIS instruments. We plot fluxes from the moment the shock was launched until it arrives at 1 AU.

Let us consider cumulative effects from the flare particles and the shock-accelerated particles (see also [2]). We run the PATH code for the same flare particles input as discussed above. Figures 3a and 4a show sharp rises in the most energetic ions of up to 100 MeV/nucleon at the beginning of the SEP event. These energetic particles are of flare origin. They contribute to the overall spectrum within the first 5 hrs. After that, their input decreases. It should be noted that a portion of the flare particles is absorbed by the shock and re-accelerated through the DSA mechanism. Thus, the flare particle still can be re-accelerated at later times. Low-energy particles start to arrive later (generally after the first 5 hrs) and their fluxes increase up to the time of an ESP event or the shock arrival time at 1 AU as seen in Figures 3b and 4b. Particles in the 44, 84 and 160 keV/nucleon energy ranges are continuously accelerated as the shock slows down. A portion of accelerated particles escapes from the evolving shock at each time step. As in the previous case, they continuously contribute to the observed flux. A portion of the low-energy particle distribution is trapped behind the shock and has a major impact on the spectrum at the shock arrival time creating an ESP event.

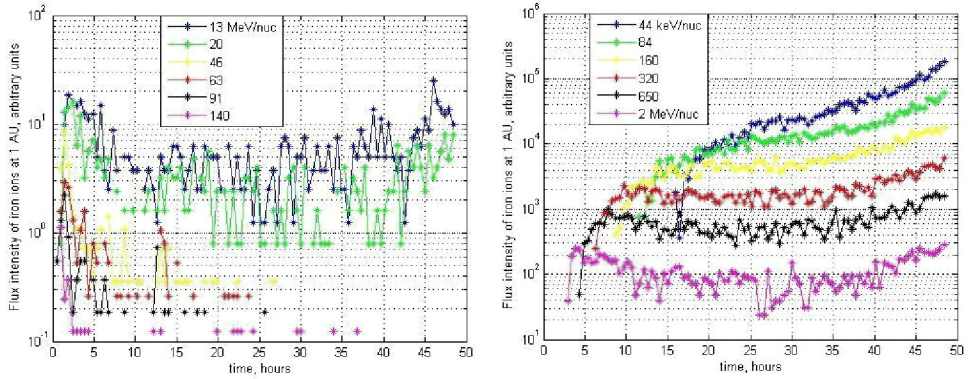


FIGURE 3. Energetic particle flux of iron ions shown in six high-energy channels (left panel) and six low-energy channels (right panel).

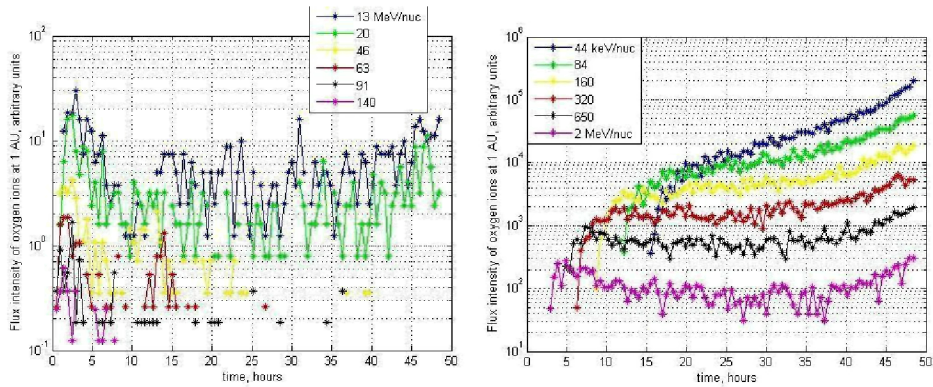


FIGURE 4. Energetic particle flux of oxygen ions shown in six high-energy channels (left panels) and six low-energy channels (right panel).

CONCLUSION

Our first modeling results show a reasonably good agreement between the modeled spectra of iron and oxygen ions and the ACE particle data. Flare particles produce a peak in fluxes measured at 1 AU during first 5 hrs of the SEP event (see Figures 3a and 4a). The high-energy particles arrive ahead of the shock which reaches the Earth's orbit in ~ 49 hrs. Lower-energy particles arrive much later (see Figures 3b and 4b). Contribution from the highest energy particles diminishes with time whereas low-energy particle fluxes increase up to the shock arrival time. The explanation is that low-energy particles are trapped in the vicinity of the shock and travel with it while being continuously

re-accelerated. Portion of these trapped particles steadily gain energy until they are able to escape from the shock and contribute to observed flux at the Earth's orbit. However, the lowest-energy particles do not escape and do not contribute to that flux until they arrive with the shock and create an ESP event. This can explain local maxima observed by SEM/GOES (see Figure 1, particle fluxes) and is reflected in our modeling results. This evolution of low- and high-energy particle fluxes agrees with the picture discussed in [1, 2].

Currently we are working to extend our 1D model to

- include a shock of an arbitrary obliquity,
- launch a shock at a radial distance of about 15 solar radii,
- incorporate different charge-to-mass ratios for flare and solar wind particles injected into the shock,
- model evolution and energy dependence of isotopic ratios of different heavy ions during the SEP event.

ACKNOWLEDGMENTS

The authors acknowledge partial support of NASA grants NNG04GF83G, NNG05GH38G, NNG05GM62G. We thank the ACE ULEIS and SIS instrument teams and the ACE Science Center for providing the ACE data. O.V. would like to thank C. Cohen, R.A. Mewaldt and E. Stone (CalTech) for stimulating discussions.

REFERENCES

1. Cane, H.V., T.T. von Rosenvinge, C.M.S. Cohen, and R.A. Mewaldt, *Geophys. Res. Lett.*, **30(12)**, 8017 (2003).
2. Li, G., and G.P. Zank, *Geophys. Res. Lett.*, **32**, L02101 (2005).
3. Li, G., G.P. Zank, and W.K.M. Rice, *J. Geophys. Res.*, 110(A06104), doi: 10.1029/2004JA010600 (2005).
4. Zank, G.P., W.K.M. Rice, and C.C. Wu, 2000, *J. Geophys. Res.*, **105(A11)**, 25079 (2000).
5. Zank, G.P., G.Li, and O.P. Verkhoglyadova, *Space Sci. Rev.*, **130**, 255, doi: 10.1007/s11214-007-9214-2 (2007).
6. Li, G., G.P. Zank, and W.K.M. Rice, *J. Geophys. Res.*, **108(A2)**, 1082, doi: 10.1029/2002JA009666 (2003).
7. Ellison, D.C., and R. Ramathy, *ApJ*, **298**, 400 (1985).
8. Mason, G. M., Gold, R. E., Krimigis, S. M., Mazur, J. E., Andrews, G. B., Daley, K. A., Dwyer, J. R., Heurman, K. F., James, T. L., Kennedy, M. J., Lefevre, T., Malcolm, H., Tossman, B., and Walpole, P. H., *Space Sci. Rev.*, **86**, 1-4, 409 (1998).
9. Stone, E. C., Cohen, C. M. S., Cook, W. R., Cummings, A. C., Gauld, B., Kecman, B., Leske, R. A., Mewaldt, R. A., Thayer, M. R., Dougherty, B. L., Grumm, R. L., Milliken, B. D., Radocinski, R. G., Wiedenbeck, M. E., Christian, E. R., Shuman, S., and von Rosenvinge, T., *Space Sci. Rev.*, **86**, Issue 1-4, 357 (1998).